COMMUNICATION

Hydrofunctionalisation of an Aromatic Triphosphabenzene

Rosalyn L. Falconer,[a] Dihao Zeng,[b] Michael Green,[a] Douglas W. Stephan,[c] John E. McGrady*[b] and Christopher A. Russell*[a]

Dedicated to the memory of Prof. Dr. Gerd Becker, an adventurer and pioneer in the field of multiply bonded phosphorus species.

Abstract: The aromatic heterocycle 2,4,6-tri-*tert*-butyl-1,3,5-triphosphabenzene reacts with a series of silanes, germanes and stannanes, with weaker E-H bonds reacting in an increasingly facile manner. All react by 1,4-addition to give bicyclic products with diastereomeric ratios varying with the substrate. Density functional theory (DFT) calculations show that activation of the E–H bond occurs across the 1,4-C/P axis of the triphosphabenzene, with the small energetic differences with respect to the stereochemistry of the addition offering insight into the experimentally observed diastereomeric ratios.

The manipulation of p-block molecules to express reactivity typically associated with transition metals has been a prominent theme in contemporary main group chemistry.[1] A range of examples of main group species capable of activating small molecules has been reported, but there are fewer examples that can demonstrate the more subtle reversible activation of bonds, which is pivotal in organo-transition metal chemistry.[2] One such example was the observation of the reversible reaction of H_2 with the ostensibly air-stable planar heterocycle 2,4,6-tri-*tert*-butyl-1,3,5-triphosphabenzene, **1**, in the absence of catalysts.[3] The only other example of reversible binding to **1**, a reversible [4+2] cycloaddition of diethyl maleate across the 1- and 4-positions of a 1,3,5-triphosphabenzene ring, was reported by Regitz *et al*.[8] DFT calculations indicated that the initial addition of the H–H bond to the C_3P_3 ring was approximately thermoneutral and had a low barrier, and indeed NMR experiments performed with *para*-hydrogen confirmed the reversibility of the H_2 addition.[7] This remarkable reactivity stands in marked contrast to analogous carbocyclic aromatic species, where H_2 activation occurs only in the presence of transition metal catalysts.[4] The computed reaction pathway for the activation of H_2 by **1** revealed the importance of the flexibility of the C_3P_3 ring, facilitating a reaction that proceeds via a boat-shaped 1,3,5-triphosphacyclohexadiene intermediate.[3a] The same boat conformation has also been observed in the ionic species **2** (Scheme 2) obtained from the reaction of **1** with $[R_3PAu]^+X^-$ (R_3P = $P(^tBu_2)$(o-biphenyl), X = SbF_6) at room temperature. DFT calculations on this cation indicate a high degree of aromaticity[6] which persists even in the absence of the gold center, highlighting the innate flexibility of the C_3P_3 ring.

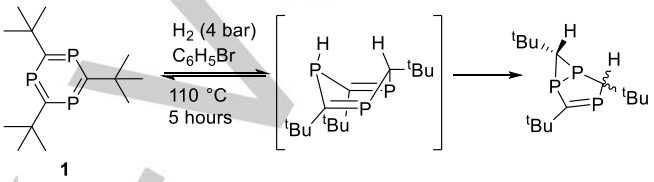

Scheme 1. Reversible activation of H_2 by 2,4,6-tri-*tert*-butyl-1,3,5-triphosphabenzene, **1**.[3a]

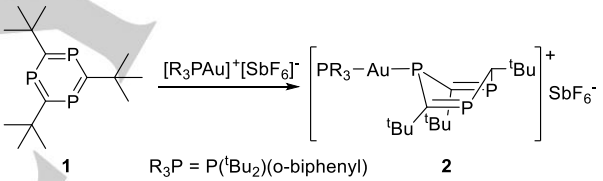

Scheme 2. Reactivity of the triphosphabenzene **1** with $[R_3PAu][SbF_6]$

It is well known that the Si–H bond in silanes is weaker than the H–H bond in H_2 due to the poorer overlap between the relevant atomic orbitals, and so it was clearly of interest to explore whether silanes, along with the related germanes and stannanes, could also be activated in a similar way by coordination to 2,4,6-tri-*tert*-butyl-1,3,5-triphosphabenzene, **1**. We were encouraged by a previous report on reduction of **1** that included the reaction between **1** and Me_3SnH which resulted in cleavage of the Sn–H bond and the formation of one bicyclic product.[9] Furthermore, if 1,4-additions do occur, then this raises two interesting questions: firstly, which orientation will the E–H bond (E = Si, Ge, Sn) adopt during activation; secondly, is the addition of the E–H bond reversible in an analogous way to the activation of H_2?

Reaction of **1** with Ph_2SiH_2 at 130 °C in C_6H_5Br gives two diastereomeric products, **3A** and **3B**, in 85 and 15% yield respectively (Scheme 3). These products are structurally analogous to the species observed upon the activation of dihydrogen by **1**: diastereotopic 3,5-fused bicyclic ring systems substituted by H and $SiPh_2H$ formed from the activation of the Si-H bond. The products were determined by their distinctive $^{31}P\{^1H\}$ NMR spectroscopic signatures and also by mass spectrometry. ^1H NMR spectroscopy revealed that in both **3A** and **3B**, the $SiPh_2H$ group is located on the 5-membered ring.

[a] Dr. C.A. Russell, Dr. R. L. Falconer, Prof. M. Green,
School of Chemistry,
University of Bristol,
Cantock's Close, Bristol, BS8 1TS, United Kingdom
E-mail: Chris.Russell@bristol.ac.uk
[b] Prof. J.E. McGrady, D. Zeng
Department of Chemistry,
University of Oxford,
South Parks Road, Oxford OX1 3QZ, United Kingdom
[c] Prof. D. W. Stephan,
Department of Chemistry,
University of Toronto,
80 St. George Street, Toronto, Ontario, M5S 3H6, Canada

Supporting information for this article is given via a link at the end of the document.

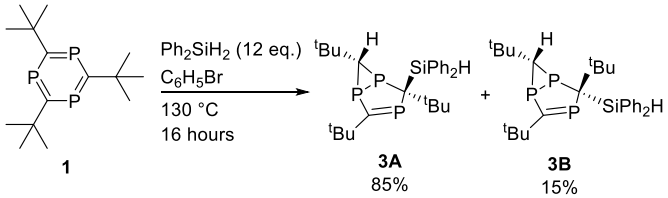

Scheme 3. Activation of diphenylsilane by **1** to form diastereomeric products **3A** and **B.**

Given this promising lead, analogous reactivity was explored with corresponding primary and tertiary silanes. Under similar conditions, reaction between **1** and the primary silane $PhSiH_3$ yielded the same two diastereomers, **4A** and **4B**, in 84% and 12% yield, along with trace amounts (2% each) of two distinct products, **4C** and **4D**, where the silane substituent is located on the 3-membered ring rather than the 5-membered one (Scheme 4, conditions in Table 1 and product ratios in Table 2). In contrast, no reaction with the tertiary silane, Ph_3SiH, was observed under analogous conditions, presumably due to the increased steric congestion around the Si–H bond. Reaction with the smaller tertiary silane $PhMe_2SiH$ was observed, although increased reactions times (40 hours) were required, leading to diastereomeric products **5A**, **5C** and **5D**. The putative isomer **5B** was not observed, while the quantities of **5C** and **5D** are marginally enhanced compared to the respective diastereomers of **4**. The corresponding reaction of Ph_2GeH_2 with **1** (125 °C, 16 h in C_6H_5Br) also afforded the two major diastereomers (**6A** and **6B**, Scheme 3 and Table 2), in approximately equal amounts, with trace amounts of diastereomers **6C** and **6D** also present. Only 1 equivalent of diphenylgermane was required for this reaction to proceed to completion overnight, indicating that activation of the Ge–H bond is more facile than that of the corresponding silane, where an excess of reagent is required (Table 1). In contrast, the stannanes $^nBu_3SnH$ and Ph_3SnH react with **1** at room temperature in C_6H_5Br to afford only a single diastereomer, **7A** and **8A** respectively (Table 2). When an excess of reagent (10 equivalents) was used, the reaction was complete in 10-15 minutes, but when stoichiometric stannane was added to **1** the reaction still proceeded at room temperature and was complete in 24 hours. The analogous reaction between **1** and Me_3SnH was reported by Jones *et al.* in 2004, which also resulted in the formation of one diastereomer only.[9][10] Tertiary tin hydrides are often used as radical initiators, but no signals attributable to radicals were observed when reactions between **1** and either $^nBu_3SnH$ or Ph_3SnH were monitored by EPR spectroscopy.[11] Similarly, these reactions remain pale yellow in color throughout the procedure, and do not show any sign of the intense coloration often associated with radical reactions. Whilst neither of these observations can rule out a radical pathway, the absence of radicals is consistent with the theoretical evidence (*vide infra*) that identifies a viable concerted pathway. We note that the increasingly mild conditions required to activate the E–H bonds (E = Si, Ge, Sn) are consistent with the decreasing E–H bond strength down Group 14.[13]

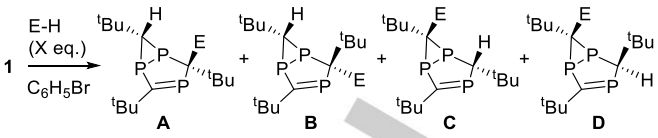

Scheme 4. General scheme for the activation of E–H bonds by **1** to form diastereomers **A**-**D**. Conditions given in Table 1 and products ratios in Table 2.

Table 1. Conditions required to activate E–H bonds by **1** as shown in Scheme 4.

Compound	E	X	Temperature (°C)	Reaction Time (h)	Yield (%)
3	$SiPh_2H$	12	130	16	100
4	$SiPhH_2$	12	130	16	100
5	$SiMe_2Ph$	12	130	40	81
6	$GePh_2H$	1	125	16	100
7	Sn^nBu_3	10	20	24	100
		1	20	0.25	100
8	$SnPh_3$	10	20	24	100
		1	20	0.17	100

Table 2. Diastereomers of products observed upon activation of E–H bonds by **1** as shown in Scheme 4.

Compound	E	Ratio of diastereomers			
		A	**B**	**C**	**D**
3	$SiPh_2H$	85	15	0	0
4	$SiPhH_2$	84	12	2	2
5	$SiMe_2Ph$	92	0	5	3
6	$GePh_2H$	49	40	7	4
7[a]	Sn^nBu_3	100	0	0	0
8[a]	$SnPh_3$	100	0	0	0

[a] Same ratio of diastereomers observed under either reaction conditions given in Table 1

Whilst it is well known that silanes can be readily activated by Lewis acids, radical mediators or transition metal species, the discovery that silanes, germanes and stannanes react with the triphosphabenzene, **1**, to give the bicyclic compounds shown in Schemes 3-5, is rather distinctive.[12] In order to explore the free energy surface for the various conceivable reaction pathways for Si–H activation, we turned to Density Functional Theory. Our initial focus was on the product selectivity, and in particular the reason why isomers **A** and **B** are formed in preference to other possibilities. There are, in fact, eight possible isomers of the product, depending on the identity of the substituent on the 3-membered ring (H, as in **A** and **B** or $SiHPh_2$, as in **C** and **D**), and on the stereochemistry at the two chiral centers. A further four

isomers, **A′**, **B′**, **C′** and **D′**, could in principle, be obtained by inverting the configuration at the carbon center of the 3-membered ring. The structures of all eight isomers and their relative free energies are summarised in Figure 1 (optimised structures are shown in supporting information, Figure S3). The optimised P–P bond lengths in the eight compounds lie in the narrow range 2.19 - 2.23 Å, consistent with the value of 2.196(1) Å found in the X-ray structure of the analogous product from the reaction with H_2. Of the eight isomers, the most stable is clearly **A**, with **B** and **C** only 3-4 kcal/mol higher in energy. In contrast **D** is somewhat higher in energy, probably due to the unfavorable steric clash between the $SiHPh_2$ and ^{t}Bu groups. The remaining four isomers, where the ^{t}Bu group on the three-membered ring is directed inwards on top of the five-membered ring, are also rather unstable, and indeed none have been observed in any of the experiments reported above.

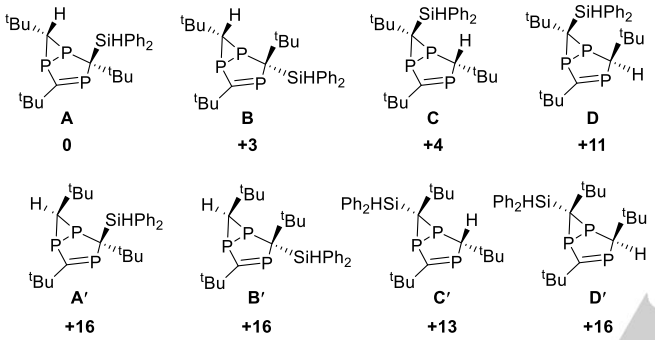

Figure 1. DFT-computed relative free energies of the eight product isomers. Energies are given in kcal/mol, relative to the most stable isomer, **A**.

The free energies shown in Figure 1, above, offer a thermodynamic rationale for the dominance of isomer **A** in all the experimental data summarised in Table 2. The fact that **B** is only marginally less stable is also consistent with its appearance as a minor product in the majority of reactions. To understand why isomer **C** is absent, given its very similar stability to **B**, we need a fuller picture of the free-energy surface for the reaction. In these calculations, the ^{t}Bu groups are replaced by the computationally more tractable Me, but the methodology is otherwise identical to that used in generating the data in Figure 1. By removing the bulk of the ^{t}Bu substituents, the steric pressure that disfavoured isomers **D**, **A′**, **B′**, **C′** and **D′** is reduced, and in fact the energies of all eight isomers are now much more similar. Nevertheless, we believe that this simplified model can shed useful light on the general features of the free-energy surface.

In our previous study of H_2 activation by **1**, we showed that in the critical transition state, the H_2 unit binds in a 1,4 mode, giving rise to the boat-shaped *cyclo*-diphospha-alkene intermediate shown in Scheme 1. Approach of an Si–H bond along the same trajectory generates two distinct pathways, one leading to the formation of C–H and P–Si bonds, the other to C–Si and P–H bonds. The free energy surface for the first of these is shown in Figure 2(a), where the intermediate, **IA**, is 7 kcal/mol more stable than the encounter complex. This intermediate can then rearrange via a 1,2 suprafacial migration of the $SiHPh_2$ group and concomitant closure of the cyclopropyl ring to yield isomer **A**, which is, as noted above, the global minimum on the surface. Alternatively, a facile inversion at the phosphorus center leads to intermediate **IB** and, ultimately, to **B** *via* a 1,2 suprafacial shift. The barriers to the two shifts ($\mathbf{TS_{IA\text{-}A}}$ and $\mathbf{TS_{IB\text{-}B}}$) are very similar, suggesting that the greater thermodynamic stability of **A** *vs* **B** is the primary reason for the excess of the former observed in most cases. The surface emanating from the alternative orientation of the Si–H bond which leads to intermediates **IC** and **ID**, both of which have P–H and C–Si bonds, is shown in Figure 2(b). Qualitatively, the surface is similar in that 1,2 suprafacial shifts, this time of a hydrogen atom, connect the intermediates to the products **C** and **D**. In this case, however, the intermediate **IC** is marginally less stable than the encounter complex, and the barriers to the hydrogen-atom shifts are much greater than those for $SiHPh_2$ shifts (~29 kcal/mol *vs* ~21 kcal/mol). As a result, isomers **C** and **D** are not accessible for kinetic reasons, even though the former has similar thermodynamic stability to the major isomers observed in solution, **A** and **B**.

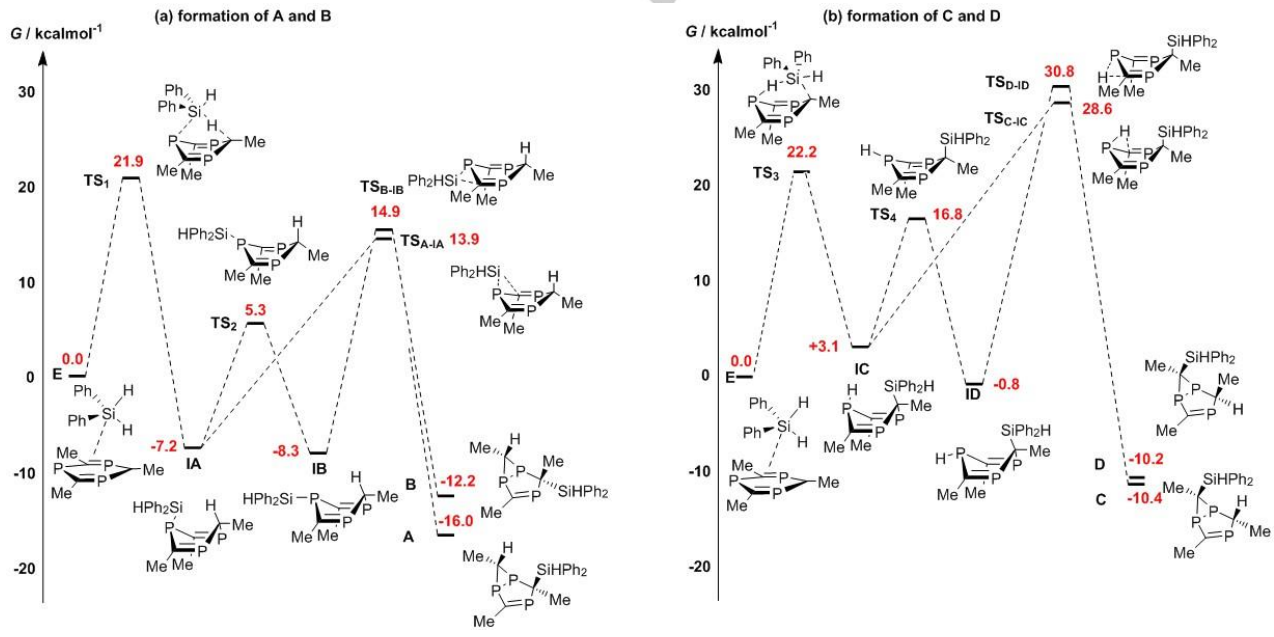

Figure 2. Free energy surfaces for Si-H activation leading to formation of (a) **A** and **B** and (b) **C** and **D**.

During the reaction of **1** with Ph_2SiH_2, one further species, **3I**, was observed in the $^{31}P\{^1H\}$ NMR spectrum, with two resonances in a 1:2 ratio (a triplet at δ -25.0 ppm and a doublet at δ 240.0 ppm). These resonances have the same distinctive spectroscopic signature as the 1,3,5-triphospha-1,4-cyclohexadiene species identified as an intermediate during the hydrogenation of **1** using ^{31}P NMR spectroscopy and *para*-hydrogen studies (Scheme 1, doublet at δ 240.0 ppm and triplet at δ -24.8 ppm). **3I** was therefore assigned as a 1,3,5-triphospha-1,4-cyclohexadiene formed from the initial addition of the Si–H bond to the 1,3,5-triphosphabenzene ring. The resonance at δ 25.0 ppm is a doublet with coupling constant of 228 Hz, indicative of a $^1J_{PH}$ coupling, which suggests that **3I** corresponds to either **IC** or **ID** rather than **IA** or **IB**. Analogous species were also observed during the reaction of **1** with Ph_2GeH_2 (**6I**), $^nBu_3SnH$ (**7I**) and Ph_3SnH (**8I**); no spectroscopic evidence for intermediates of structure corresponding to **IA** or **IB** has been observed in any of these reactions. Figure 2(b) suggests that **ID** is the more likely candidate for **3I** because it is marginally more stable than **IC**. The fact that **3I** can be observed suggests that it lies in a fairly deep well in the free energy surface, and indeed we see that the barrier for rearrangement of **ID** to **D** is 31.6 kcal/mol. In contrast, the more facile $SiHPh_2$ migration via $\mathbf{TS_{A\text{-}IA}}$ and $\mathbf{TS_{B\text{-}IB}}$, with barriers of 23.2 and 21.1 kcal/mol, respectively, means that neither **IA** nor **IB** is likely to have a lifetime sufficient to allow detection on the NMR timescale.

At the completion of the reaction of **1** with SiH_2Ph_2, all traces of the signals for **3I** had disappeared, leaving only the major products **3A** and **3B**. Similar observations were made for **7** and **8**: although **7I** and **8I** were detected as intermediates, the final product distribution contains only **7A** and **8A**. This observation suggests either that the initial addition of SiH_2Ph_2 to form **ID** is reversible, or that there is another pathway that connects the two sides of Figure 2 (a and b), allowing for the direct interconversion of **C**/**D** to **A**/**B**. Moreover, when solutions of either **7A** or **8A** in C_6D_5Br were heated for 24 hours at 130 °C, we observe the formation of significant quantities of **B**, but also smaller amounts of **C** and **D** (Scheme 5). The relatively facile interconversion of **A** and **B** can be achieved *via* a combination of 1,2 suprafacial migration of SnR_3 and phosphine inversion, which allows for the interconversion of the two isomers *via* **IA** and **IB** with barriers of the order of 20 kcal/mol. The appearance of **C** and **D**, albeit in rather small quantities, requires either that Sn–H activation is reversible and that the encounter complex can be regenerated, or, again, that there is another pathway that allows for direct interconversion of **A**/**B** to **C**/**D**.

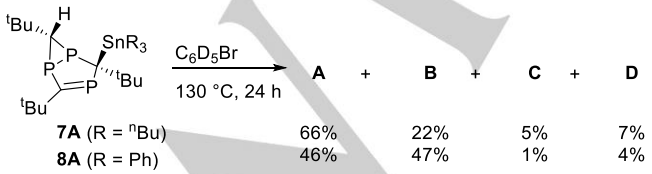

Scheme 5. Interconversion of **7A** and **8A** to diastereomers **A-D** at elevated temperatures

The direct transformation from **A/B** to **C/D** and vice versa involves the scrambling of the substituents on the three- and five-membered rings, a process which can, in principle, be achieved *via* a phosphorus analogue of the "vinyl-cyclopropyl to cyclopentadiene" rearrangement (Figure 3). The mechanism of the all-carbon analogue of this reaction has been studied extensively, by Houk and Davidson,[14] who report that the key transition state is a biradical species containing weakly coupled carbon and allyl radical centers. We have been able to locate four very similar transition states, interconverting **B↔D ($\mathbf{TS_{BD}}$), A↔D′ ($\mathbf{TS_{AD'}}$), A′↔C′ ($\mathbf{TS_{A'C'}}$)** and **B′↔C ($\mathbf{TS_{B'C}}$)**, shown in Figure 3. Isomers **A** and **C** are connected to high-energy isomers where the ^{t}Bu group lies over the five-membered ring (**D′** and **A′**, respectively), but this pathway does provide a plausible mechanism for the interconversion or **B** to **D** and *vice versa*. The transition structure $\mathbf{TS_{BD}}$ has an approximately C_2-symmetric 6-membered C_3P_3 ring with one electron localised on one P center and another delocalised over a P-CMe-P allyl-like unit: the value of $\langle S^2 \rangle$ = 1.01 is highly diagnostic of an open-shell singlet, as seen in the all-carbon analogue.[16] The barrier to direct interconversion of **B** to **D** via $\mathbf{TS_{BD}}$ is 33.1 kcal/mol, compared to a maximum barrier of 43.0 kcal/mol (**B** to $\mathbf{TS_{D\text{-}ID}}$) for the completely reversible reaction *via* the encounter complex, **E**.

On balance, although it is tempting to posit reversibility, we are unable to do so definitely with current evidence; further experiments will be required to unravel these most interesting observations.

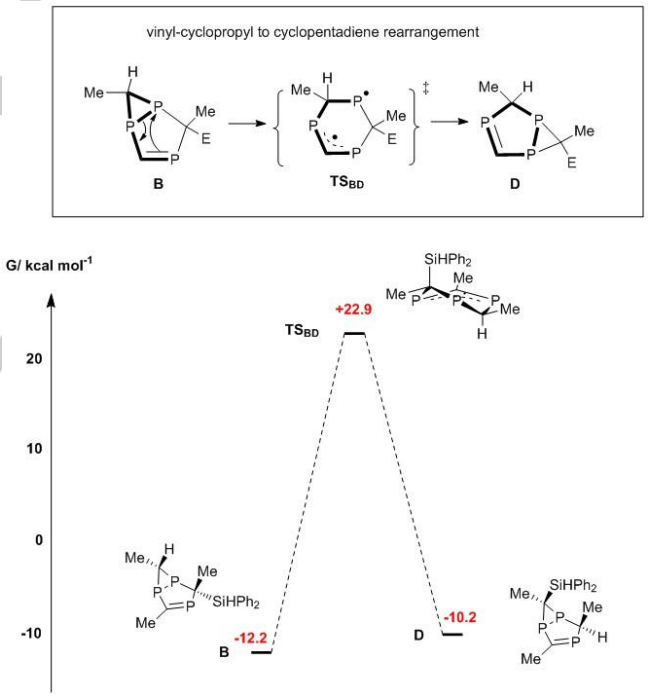

Figure 3. The vinyl-cyclopropene to cyclobutadiene pathway for the direct interconversion of **B** and **D**.

In conclusion, the scope of small molecule activation by the aromatic heterocycle 1,3,5-triphosphabenzene, **1**, has been extended beyond H_2 to include a range of E–H bonds (E = Si, Ge, Sn). Calculations performed at the DFT level indicate that these reactions follow a similar pathway to the activation of dihydrogen, but with additional stereo-chemical implications which arise from the asymmetry of the bond being activated.

Computational methods

All calculations were performed using density functional theory as implemented in the Gaussian16 software package.[15] The dispersion-corrected ωB97D functional[16] was used throughout, in conjunction with Ahlrichs' def2-TZP basis set on nine core atoms (the C_3P_3 ring and the SiH_2 unit).[17] The remainder of the molecule was described by the more tractable def2-SV basis set. In the initial calculations of the stabilities of isomers **A**, **A′**, **B**, **B′**, **C**, **C′**, **D** and **D′**, the full ^{t}Bu group was used but for the study of the free energy surfaces they were replaced by Me groups. All stationary points were confirmed as minima/transition states by the absence/presence of a single imaginary vibrational frequency. The reported free energies (298 K) contain corrections for the zero-point energy as well as entropies.

Acknowledgements

RLF thanks the Bristol Chemical Synthesis Centre for Doctoral Training, funded by EPSRC (EP/G036764/1), and the University of Bristol, for a PhD studentship. We thank the EPSRC UK National Mass Spectrometry Facility at Swansea University.

Keywords: metal free • triphosphabenzene • hydrosilylation • hydrofunctionalisation • phosphorus

[1] a) P. P. Power, *Nature* **2010**, *463*, 171; b) C. Weetman, S. Inoue, *ChemCatChem* **2018**.
[2] Examples include: a) D. W. Stephan, *Org. Biomol. Chem.* **2008**, *6*, 1535; b) S. K. Mandal, H. W. Roesky, *Acc. Chem. Res.* **2012**, *45*, 298; c) C. D. Martin, M. Soleilhavoup, G. Bertrand, *Chem. Sci.* **2013**, *4*, 3020; d) D. W. Stephan, G. Erker, *Angew. Chem., Int. Ed.* **2015**, *54*, 6400; e) S. Yadav, S. Saha, S. S. Sen, *ChemCatChem* **2015**, *8*, 486; f) D. W. Stephan, Science **2016**, *354*, aaf7229; g) M. Melaimi, R. Jazzar, M. Soleilhavoup, G. Bertrand, *Angew. Chem., Int. Ed.* **2017**, *56*, 10046; h) T. Sugahara, J. D. Guo, T. Sasamori, S. Nagase, N. Tokitoh, *Angew. Chem., Int. Ed.* **2018**, *57*, 3499; i) S. Wang, T. J. Sherbow, L. A. Berben, P. P. Power, *J. Am. Chem. Soc.* **2018**, *140*, 590.
[3] a) L. E. Longobardi, C. A. Russell, M. Green, N. S. Townsend, K. Wang, A. J. Holmes, S. B. Duckett, J. E. McGrady, D. W. Stephan, *J. Am. Chem. Soc.* **2014**, *136*, 13453; b) R. L. Falconer, C. A. Russell, *Coord. Chem. Rev.* **2015**, *297-298*, 146; c) D. W. Stephan, *Acc. Chem. Res.* **2015**, *48*, 306.
[4] F. Joó in *Science of Synthesis: Water in Organic Synthesis, Vol. 1*, Thieme Chemistry, **2012**.
[5] N. S. Townsend, M. Green, C. A. Russell, *Organometallics* **2012**, *31*, 2543.
[6] P. v. R. Schleyer, C. Maerker, A. Dransfeld, H. Jiao, N. J. R. van Eikema Hommes, *J. Am. Chem. Soc.* **1996**, *118*, 6317.
[7] R. W. Adams, J. A. Aguilar, K. D. Atkinson, M. J. Cowley, P. I. P. Elliott, S. B. Duckett, G. G. R. Green, I. G. Khazal, J. López-Serrano, D. C. Williamson, *Science* **2009**, *323*, 1708.
[8] C. Peters, H. Disteldorf, E. Fuchs, S. Werner, S. Stutzmann, J. Bruckmann, C. Kruger, P. Binger, H. Heydt, M. Regitz, *Eur J Org Chem* **2001**, 3425.
[9] C. Jones, M. Waugh, *Dalton Trans.* **2004**, 1971.
[10] The topology of the assigned molecule is consistent with the data herein, but, based on the more extensive data in this report, we suspect that the assignment of the specific diastereomer is incorrect.
[11] D. P. Curran, *Synthesis* **1988**, *1988*, 417.
[12] Examples include: a) D. Mukherjee, D. F. Sauer, A. Zanardi, J. Okuda, *Chem. - Eur. J.* **2016**, *22*, 7730; b) V. Fasano, J. E. Radcliffe, L. D. Curless, M. J. Ingleson, *Chem. - Eur. J.* **2017**, *23*, 187; c) Y. Ma, B. Wang, L. Zhang, Z. Hou, *J. Am. Chem. Soc.* **2016**, *138*, 3663; d) A. Y. Houghton, J. Hurmalainen, A. Mansikkamäki, W. E. Piers, H. M. Tuononen, *Nat Chem* **2014**, *6*, 983; e) C. Chatgilialoglu, *Acc. Chem. Res.* **1992**, *25*, 188; f) M. Tojino, N. Otsuka, T. Fukuyama, H. Matsubara, C. H. Schiesser, H. Kuriyama, H. Miyazato, S. Minakata, M. Komatsu, I. Ryu, *Org. Biomol. Chem.* **2003**, *1*, 4262; g) R. J. Trovitch, *Acc. Chem. Res.* **2017**, *50*, 2842; h) X. Du, Z. Huang, *ACS Catalysis* **2017**, *7*, 1227; i) M. Oestreich, *Angew. Chem., Int. Ed.* **2016**, *55*, 494; j) M. Oestreich, *Angew. Chem.* **2016**, *128*, 504.
[13] J. A. Dean, N. A. Lange in *Lange's Handbook of Chemistry*, 13th ed., McGraw-Hill, USA, **1992**.
[14] (a) K.N. Houk, M. Nendel, O. Wiest and J.W. Storer, *J. Am. Chem. Soc*., **1997**, 119, 10545. (b) E. R. Davidson and J. J. Gajewski, *J. Am. Chem. Soc*., **1997**, 119, 10543.
[15] Gaussian 16, Revision A.03, M. J. Frisch, G. W. Trucks, H. B. Schlegel, G. E. Scuseria, M. A. Robb, J. R. Cheeseman, G. Scalmani, V. Barone, G. A. Petersson, H. Nakatsuji, X. Li, M. Caricato, A. V. Marenich, J. Bloino, B. G. Janesko, R. Gomperts, B. Mennucci, H. P. Hratchian, J. V. Ortiz, A. F. Izmaylov, J. L. Sonnenberg, D. Williams-Young, F. Ding, F. Lipparini, F. Egidi, J. Goings, B. Peng, A. Petrone, T. Henderson, D. Ranasinghe, V. G. Zakrzewski, J. Gao, N. Rega, G. Zheng, W. Liang, M. Hada, M. Ehara, K. Toyota, R. Fukuda, J. Hasegawa, M. Ishida, T. Nakajima, Y. Honda, O. Kitao, H. Nakai, T. Vreven, K. Throssell, J. A. Montgomery, Jr., J. E. Peralta, F. Ogliaro, M. J. Bearpark, J. J. Heyd, E. N. Brothers, K. N. Kudin, V. N. Staroverov, T. A. Keith, R. Kobayashi, J. Normand, K. Raghavachari, A. P. Rendell, J. C. Burant, S. S. Iyengar, J. Tomasi, M. Cossi, J. M. Millam, M. Klene, C. Adamo, R. Cammi, J. W. Ochterski, R. L. Martin, K. Morokuma, O. Farkas, J. B. Foresman, and D. J. Fox, Gaussian, Inc., Wallingford CT, **2016**.
[16] J.-D. Chai and M. Head-Gordon, *Phys. Chem. Chem. Phys.*, **2008**, 10, 6615.
[17] F. Weigend and R. Ahlrichs, *Phys. Chem. Chem. Phys.*, **2005**, 7, 3297.

Entry for the Table of Contents

COMMUNICATION

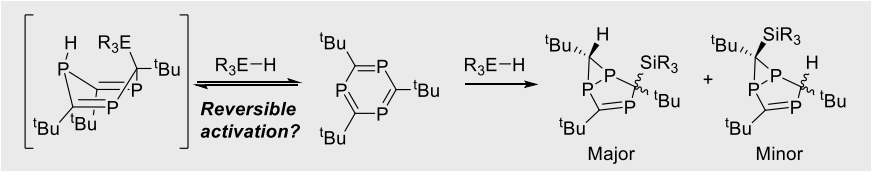

The aromatic heterocycle 2,4,6-tri-*tert*-butyl-1,3,5-triphosphabenzene reacts with silanes, germanes and stannanes by initial 1,4-addition and subsequent rearrangement to give bicyclic products with diastereomeric ratios that vary with the substrate.

*Rosalyn L. Falconer, Dihao Zeng, Michael Green, Douglas W. Stephan, John E. McGrady, Christopher A. Russell**

Page No. – Page No.

Hydrofunctionalisation of an Aromatic Triphosphabenzene